



HAL
open science

Modal Characterization of Manual Wheelchairs

Ophélie Lariviere, Delphine Chadefaux, Christophe Sauret, Layla Kordulas,
Patricia Thoreux

► **To cite this version:**

Ophélie Lariviere, Delphine Chadefaux, Christophe Sauret, Layla Kordulas, Patricia Thoreux. Modal Characterization of Manual Wheelchairs. *Vibration*, 2022, 5 (3), pp.442-463. 10.3390/vibration5030025 . hal-03758480

HAL Id: hal-03758480

<https://hal.science/hal-03758480v1>

Submitted on 23 Aug 2022

HAL is a multi-disciplinary open access archive for the deposit and dissemination of scientific research documents, whether they are published or not. The documents may come from teaching and research institutions in France or abroad, or from public or private research centers.

L'archive ouverte pluridisciplinaire **HAL**, est destinée au dépôt et à la diffusion de documents scientifiques de niveau recherche, publiés ou non, émanant des établissements d'enseignement et de recherche français ou étrangers, des laboratoires publics ou privés.

Article

Modal Characterization of Manual Wheelchairs

Ophélie Larivière ^{1,2,*}, Delphine Chadeaux ^{1,2} , Christophe Sauret ^{3,4} , Layla Kordulas ⁴ and Patricia Thoreux ^{1,5}

- ¹ Institut de Biomécanique Humaine Georges Charpak, IBHGC, Université Sorbonne Paris Nord, UR 4494, F-93000 Bobigny, France; delphine.chadeaux@sorbonne-paris-nord.fr (D.C.); patricia.thoreux@aphp.fr (P.T.)
- ² Département STAPS, Université Sorbonne Paris Nord, F-93000 Bobigny, France
- ³ Arts et Métiers Institute of Technology, Institut de Biomécanique Humaine Georges Charpak, IBHGC, UR 4494, F-75013 Paris, France; christophe.sauret@ensam.eu
- ⁴ Centre d'Etudes et de Recherche sur l'Appareillage des Handicapés, Institution Nationale des Invalides, F-94000 Créteil, France; layla.kordylas@edu.supmeca.fr
- ⁵ Hôpital Hôtel Dieu, AP-HP, F-75004 Paris, France
- * Correspondence: ophelie.lariviere@sorbonne-paris-nord.fr

Abstract: Manual wheelchair (MWC) users are exposed to whole-body vibrations (WBVs) during propulsion. Vibrations enter the MWC structure through the wheels' hub, propagate according to the MWC dynamical response, and finally reach the user's body by the footrest, seat, backrest, and handrims. Such exposure is likely to be detrimental to the user's health and a source of discomfort and fatigue which could, in daily life, impact users' social participation and performance in sports. To reduce WBV exposure, a solution relies on MWC dynamical response modelling and simulation, where the model could indeed be used to identify parameters that improve the MWC dynamic. As a result, it is necessary to first assess the MWC dynamical response. In this approach, experimental modal analyses were conducted on eleven MWCs, including daily and sport MWCs (tennis, basketball, and racing). Through this procedure, modal properties (i.e., modal frequencies, damping parameters, and modal shapes) were identified for each MWC part. The results pointed out that each MWC investigated, even within the same group, revealed specific vibration properties, underlining the difficulty of developing a single vibration-reducing system for all MWCs. Nevertheless, several common dynamical properties related to MWC comfort and design were identified.

Keywords: manual wheelchair; modal analysis; hammer roving test



Citation: Larivière, O.; Chadeaux, D.; Sauret, C.; Kordulas, L.; Thoreux, P. Modal Characterization of Manual Wheelchairs. *Vibration* **2022**, *5*, 442–463. <https://doi.org/10.3390/vibration5030025>

Academic Editor: Paul-Émile Boileau

Received: 31 May 2022

Accepted: 19 July 2022

Published: 21 July 2022

Publisher's Note: MDPI stays neutral with regard to jurisdictional claims in published maps and institutional affiliations.



Copyright: © 2022 by the authors. Licensee MDPI, Basel, Switzerland. This article is an open access article distributed under the terms and conditions of the Creative Commons Attribution (CC BY) license (<https://creativecommons.org/licenses/by/4.0/>).

1. Introduction

The health and social integration of people with disabilities are current social issues. When using a manual wheelchair (MWC), ground/wheel interactions induce MWC vibrations that are transmitted to the user. Depending on the exposure time, frequency content, and amplitude, the generated vibrations can affect human health and comfort. Indeed, epidemiological studies have found that workers exposed on a daily basis to whole-body vibrations, such as bus and truck drivers, are more prone to suffer from lower back [1,2] and neck pains [3], which could be explained by the deterioration of the intervertebral discs [4]. Furthermore, vibrations tend to increase reaction time [5] and alter both vision and balance [6,7], affecting human well-being. Under this framework, guidelines were developed for workers' health protection, such as the European directive 2002/44/EC [8] and the ISO-2636-1 standard (mechanical vibration and shock, evaluation of human exposure to whole-body vibrations), which fixed the maximum vibration exposure based on vibration frequencies in the deleterious human body frequency range (i.e., [4–80 Hz] with a particular risk between 4 and 12 Hz for the seated human body) [9]. For that purpose, an acceptable maximal vibration dose of $0.5 \text{ m}\cdot\text{s}^{-2}$ was recommended for an eight-hour exposure, beyond which health could be affected. Although no study has yet been carried out linking the pathologies of MWC users to their exposure to vibrations, MWC users' daily exposure to vibrations exceeds the ISO-2631 recommendations (i.e., $0.83 \text{ m}\cdot\text{s}^{-2}$) [10].

In addition, a prevalence of neck and lower back pains was observed in the MWC user population [10]. In addition, besides the vibration dose, the spectral content transmitted to the user has to be assessed and kept out from frequency ranges that are harmful to anatomical structures.

In addition to the health risks, vibrations can also affect MWC lifetime and function. At a given set of excitation frequencies (i.e., MWC eigenfrequencies), interactions between the inertial and elastic properties of the structure materials cause a resonance phenomenon [11]. In the long term, the repetition of the local deformations induced by the resonance phenomenon can cause cracks, loose screws, bolts, mechanical fatigue, or even failure of the MWC [12].

To protect the user and preserve the MWC lifetime, a dynamic model of the MWC needs to be used. As the characteristics of the WBV reaching the MWC user depends on both the user (e.g., their morphology, posture, and muscular activation) and the MWC dynamical behaviour [13,14], modifying an MWC setting/parameter rarely shows systematic effects on WBV exposure. To address this issue, one solution is to develop a dynamic model of the MWC/user dyad exposed to vibration. Until now, only a few authors have tried to model the vibration transmissibility during MWC propulsion [13,15–17]. Except for Mastuoka et al. [13,17], most studies have focused on a mechanical model of the seated able-bodied human [6], neglecting the MWC. The model proposed by Mastuoka et al. [13,17] considers the MWC as a single rigid body, preventing a parametric study of the MWC settings. By using a parametric model of the MWC, it is possible to account for the individual vibration response of each MWC/user dyad.

Building such a model first requires knowledge of the MWC dynamical behaviour. Skendraoui et al. [18] estimated the eigenmodes of an isolated standard MWC through experimental modal analysis and finite element analysis. Although modal damping ratios are useful for MWC model input, Skendraoui et al. [18], unfortunately, did not report them. Furthermore, to meet the needs of MWC users, manufacturers have developed many variations of MWC designs, modifying the MWC structure, the materials, the components (e.g., the type of wheels), etc. It is, therefore, necessary to investigate whether such modifications affect MWC modal properties.

The present study aims to provide data on the dynamical behaviour of very different MWC types. Such knowledge is needed for the implementation of an MWC mechanical model. This information, which identifies the frequencies at which vibrations are amplified by the MWC, can also assist MWC manufacturers in the development or the improvement of accessories to reduce vibration exposure. Indeed, currently, to damp shock and continuous vibrations, suspensions can be added to the MWC, for instance. However, although suspensions have proven to be efficient for shock absorption [19], they are ineffective at reducing the vibration transmission in the frequency range that is deleterious for the human body (i.e., [4–80 Hz] [9]). Beyond modifying the MWC structure, specific equipment can be used to protect the human body from WBVs (e.g., cushion, gloves). These modifications to the equipment must be designed to take into account its dynamical response [20]. Indeed, unexpectedly, cushions generally amplify the amplitude of vibrations in the [4–80 Hz] frequency range [16,21], considered as deleterious for the human body [6].

One way to obtain dynamical properties is experimental modal analysis. Such a method consists of observing the dynamic response of a structure to a known disturbance. The disturbance is generally obtained thanks to an instrumented hammer or a shaker. The structure response is generally measured with an accelerometer [11]. Additionally, non-invasive methods based on 3D laser vibrometry also exist [22]. Such non-invasive methods have the advantage of generating a disturbance and measuring the structure response without affecting the structure, which is particularly interesting for very light structures. However, they need more experimental equipment that prevents measurements outside the laboratory. For this reason and given the MWC size, experimental modal analyses were conducted with the roving hammer method (EMA) [23]. Such measurements were performed in the [4–80 Hz] frequency range and on eleven MWCs, including both daily

(i.e., lightweight and standard) and sports (i.e., tennis, basketball, and racing) MWCs. A secondary goal was to estimate the variability of the MWC modal properties (the frequency and damping ratio) across the set of investigated MWCs. Such information will be useful to know if it is necessary to characterize all the MWCs or if some trends could be observed between two similar MWCs. The main hypothesis of this study was that MWCs of a same type would result in similar dynamical behaviour, whereas differences were expected between different types of MWCs, especially for racing MWCs, which have a particular frame shape.

2. Materials and Methods

2.1. Manual Wheelchairs

The experimental modal analysis (EMA) of eleven manual wheelchairs (MWCs) without cushions, whose mechanical characteristics are provided in Table 1 and photo in Appendix A, was performed.

Table 1. Manual wheelchairs specification. Geometrical and inertial properties of the MWC were obtained through methods described in [24–26]. NA means that the properties could not be obtained.










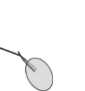












Type	Daily				Sport							
	Lightweight		Standard		Basketball	Tennis		Racing				
Photo												
Name	MWC01	MWC02	MWC03	MWC04	MWC05	MWC06	MWC07	MWC08	MWC09	MWC10	MWC11	
Model	Ottobock Voyager Evo	Invacare Kuschall KSL	Vermeiren Eclips +30°	Vermeiren D200	Ottobock Invader sport	Sunrise Grand Slam	Tailor-made manufacturing	Invacare Top end	Invacare Top end	Invacare Top end	Invacare Top end	
Photo												
Folding			x	x								
Frame material	Al	Al	Al	Al	Al	Al	C	Al	Al	C	C	
Masse [kg]	12	9	19	17	12	10	11	10	9	9	8	
Moment of inertia [kg.m ²]	1	1	2	3	1	1	1	2	2	2	2	
Centre of mass [cm]	X (front)	16	11	20	8	9	2	5	29	26	23	22
	Y (height)	31	33	42	32	30	35	26	38	41	42	41
	Z (lateral)	1	1	0	0	0	0	−4	0	−1	0	0
Configuration	Seat width [cm]	38	37	42	52	34	38	NA	25	22	32	22
	Seat depth [cm]	39	45	45	43	34	36	NA	38	37	18	9
	Seat front height [cm]	49	48	50	50	50	47	56	44	49	48	53
	Seat back height [cm]	42	41	49	50	45	49	56	46	49	45	56
	Seat advanced [cm]	−8	−11	8	−4	−8	16	NA	−7	−11	NA	NA
Configuration	Backrest angle [°]	8	2	6	17	5	5	NA	25	2	NA	NA
	Wheel camber [°]	4	3	1	1	15	23	20	13	12	11	11
	Front wheel radius [cm]	7	6	10	10	4	4	8	24	24	23	23
	Back wheel radius [cm]	30	30	31	31	30	32	34	33	33	33	34

Table 1. Cont.

Handrim radius [cm]	26	26	27	27	27	29	32	20	19	19	17
Wheel base [cm]	40	41	50	50	38	36	37	131	120	133	129
Back wheel gap [cm]	61	58	65	72	67	77	67	51	51	49	52

During the measurement, each MWC was supported on strings to analyse it under free boundary conditions (Figure 1). The EMA procedure aims to identify mode shapes, eigenfrequencies, and damping factors from the frequency response functions (FRFs) measured on each MWC part. The MWC parts were defined according to the typical MWC elements: the seat, backrest, footrest, frame, side guard, rear wheel, and handrim. Depending on the investigated MWC part’s geometry, the EMA was performed in one, two, or three directions. The MWC parts and directions studied with respect to the MWC frame of reference are reported Table 2.

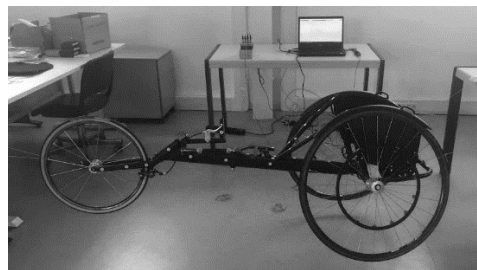
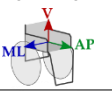
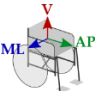

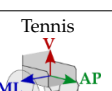
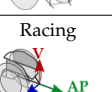


Figure 1. Picture of the experimental setup.

Table 2. Parts and direction studied for each MWC. When side guards, backrest, and footrest were not investigated, it was because the MWC did not have any. The seat was not studied on the racing MWC08 because the two beams on which tensors were stretched were not accessible in the vertical direction. Rear wheel of standard MWC03 was not observed due to a lack of time regarding the MWC availability.

MWC Part	Direction	Frame			Side Guards	Backrest		Seat	Footrest	Rear Wheel	Handrim
		V	ML	AP	ML	ML	AP	V	V	ML	ML
Lightweight											
	MWC01	X		X		X	X	X	X	X	X
	MWC02	X		X	X	X	X	X	X	X	X
Standard											
	MWC03	X	X		X	X	X	X	X		X
	MWC04	X	X		X	X	X	X	X	X	X
Basketball											
	MWC07	X	X		X	X	X	X	X	X	X
Tennis											
	MWC05	X	X		X	X	X	X	X	X	X
	MWC06	X	X					X		X	X
Racing											
	MWC08	X	X		X					X	X
	MWC09	X	X		X			X		X	X
	MWC10	X	X		X			X		X	X
	MWC11	X	X		X			X		X	X

2.2. Mesh

The FRFs were measured on a mesh of 70 to 170 points, depending on the MWC, distributed over the whole MWC structure. Each mesh point was highlighted by coloured stickers fixed to the MWC part. To determine the coordinates of each mesh point, a 3D scan was performed (iSense iPad 4G, 3D Systems) to obtain a coloured 3D model of the MWC. Based on this model, a MATLAB routine was developed to extract 3D coordinates of the impact points from the 3D mesh through a selecting and colour identification procedure.

2.3. Experimental Modal Analysis

Force data were segmented using a uniform 10 ms rectangular window centred on the hammer impact. An exponential decay window was applied to the acceleration signals to reduce leakage [11]. The quality of the data was then verified using the coherence function [11]. To obtain the eigenfrequencies, damping ratios, and mode shapes, the FRFs, H_{ij} , were calculated as:

$$H_{ij}(f) = \frac{A_{ij}(f)}{F_i(f)} \quad (1)$$

where f is the frequency vector, A_{ij} is the acceleration measured by the accelerometer j for an impact in point i , and F_i is the impact force at point i . The FRFs were analysed between 4 and 80 Hz, according to the seated human body's sensitivity response to vibration [6].

To calculate the FRFs, each mesh point was successively excited with an impact hammer (086C02, PCB Piezotronics, $11.2 \text{ mV} \cdot \text{N}^{-1}$, $\pm 444 \text{ N} \cdot \text{pk}$, resonant frequency $\geq 15 \text{ kHz}$, sampling rate 25,600 Hz). The excitation was repeated as many times as required to obtain a force signal with an acceptable bandwidth (i.e., a band limit higher than 200 Hz), a low noise level, and no secondary impact. The resulting normal acceleration was measured by one synchronized mono-axial accelerometer (352A24 Accelerometer, ICP[®], PCB Piezotronics, Buffalo, NY, USA, $100 \text{ mV} \cdot \text{g}^{-1}$, $\pm 50 \text{ g} \cdot \text{pk}$, [1–8000 Hz], sampling rate 25,600 Hz) fixed on the part studied and aligned in the direction of interest.

For each MWC part, the frequencies were firstly visually identified (i.e., the FRF phase change associated with an FRF peak). Based on the identified frequencies, the modal properties were identified using the Least Squared Complex Frequency domain (LSCF) method [12,23] implemented in the Structural Dynamic Toolbox [23] running on MATLAB R2019b. The modal properties were obtained through an iterative local estimation around each pole. The modes were excluded if the contribution level and Modal Phase Collinearity (MPC) were lower than 10%, the noise level was higher than 10%, and the identification error was higher than 10%.

3. Results

Table 3 presents the modal parameters obtained for each of the studied MWC parts. The results are detailed by parts in the next sections.

Table 3. MWC modal parameters (eigenfrequencies (Fo), damping ratios (ξ_o) and amplitude (Amp)) for each part studied. Grey boxes mean that the part was not studied for the MWC and empty boxes mean no mode was observed between 4 and 80 Hz.

	Lightweight									Standard			Basketball			Tennis			Racing																		
	MWC01			MWC02			MWC03			MWC04			MWC05			MWC06			MWC07			MWC08			MWC09			MWC10			MWC11						
	Fo (Hz)	ξ_o (%)	Amp	Fo (Hz)	ξ_o (%)	Amp	Fo (Hz)	ξ_o (%)	Amp	Fo (Hz)	ξ_o (%)	Amp	Fo (Hz)	ξ_o (%)	Amp	Fo (Hz)	ξ_o (%)	Amp	Fo (Hz)	ξ_o (%)	Amp	Fo (Hz)	ξ_o (%)	Amp	Fo (Hz)	ξ_o (%)	Amp	Fo (Hz)	ξ_o (%)	Amp	Fo (Hz)	ξ_o (%)	Amp				
V	17	5	5×10^2	25	5	2×10^2	13	6	3×10^2	21	3	6×10^3	10	6	7×10^2	17	7	2×10^2	29	7	1×10^3	18	3	3×10^3	29	2	3×10^2	27	4	3×10^3	33	4	9				
	36	3	2×10^3	35	3	1×10^3	17	4	3×10^3	31	4	2×10^3	18	4	6×10^2	44	3	2×10^3	37	3	3×10^3	45	2	2×10^3	49	1	2×10^3	42	3	2×10^3	66	4	6				
	44	3	2×10^3	46	3	3×10^3	25	5	3×10^3	42	4	8×10^2	73	4	3×10^2	55	3	1×10^3	51	7	8×10^2	51	2	5×10^2	55	2	6×10^2	47	2	1×10^3	74	3	6				
	60	2	2×10^3	57	2	2×10^4	28	3	8×10^3							62	3	1×10^3	79	2	6×10^3	53	3	1×10^2				53	4	3×10^2							
	66	2	2×10^3	61	4	1×10^4	35	5	1×10^3																												
							40	3	4×10^3																												
							44	3	4×10^3																												
							74	3	4×10^3																												
	ML							16	7	5×10^3	64	5	6×10^2	34	2	1×10^4	18	6	6×10^2	49	3	8×10^2	28	2	1×10^2	29	2	1×10^2	35	2	1×10^3	41	2	1×10^2			
								19	5	2×10^3	77	3	7×10^2	50	3	1×10^4	72	7	8×10^3				39	1	1×10^3	49	1	2×10^3	43	3	1×10^4	59	1	1×10^2			
								22	4	2×10^3				73	5	8×10^2							51	2	2×10^2	55	2	3×10^3	48	2	6×10^3						
								28	3	1×10^4																60	2	9×10^2	58	2	1×10^4	52	2	1×10^3			
								30	3	2×10^4																77	2	3×10^2	67	2	2×10^3	55	2	7×10^2			
								35	3	4×10^3																						56	1	5×10^2			
								45	3	3×10^3																						73	2	2×10^3			
							49	4	3×10^2																												
						76	4	1×10^3																													
AP	16	5	1×10^2	25	5	1×10^2																															
	38	2	1×10^3	35	7	7×10^2																															
	43	4	2×10^2	61	5	3×10^2																															
	64	1	2×10^4																																		
ML				49	2	7	9	8	7×10^4	48	2	9	15	5	3×10^3	44	2	1×10^3				15	6	6×10^2	17	6	6×10^2	35	2	9×10^3	33	6	1×10^3				
							35	2	5×10	75	9	4	70	3	1×10^2	57	9	4×10^2				29	2	1×10^3	29	2	2×10^3	42	2	2×10^3	41	2	2×10^3				
							44	3	3×10													45	2	1×10^3	49	1	2×10^3	52	2	1×10^2	54	2	2×10^2				
																						51	2	2×10^3	59	2	4×10^2										
																						60	2	1×10^2	68	2	6×10										
																						77	2	8×10^2													

3.1. Frame

Figure 2 illustrates the co-located FRF and the eigenmodes identified at the frame of the eleven MWCs along all the directions studied. In the next part, for readability purposes, the results are presented as the mean (standard deviation).

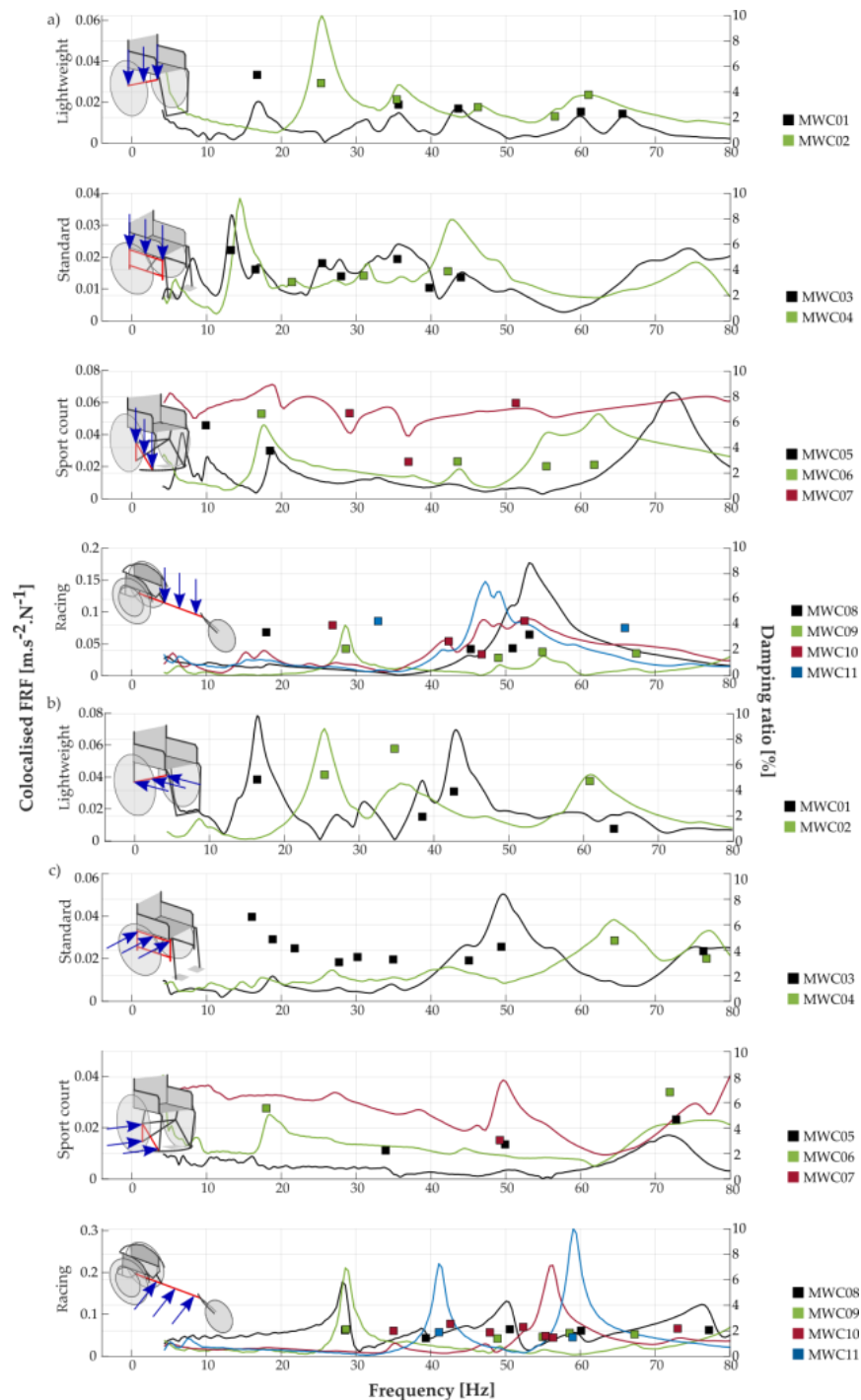


Figure 2. Co-located FRF (lines, associated with the left *y*-axis) and eigenmodes (squared markers, associated with the right *y*-axis) of the frame for each MWC type and direction studied (a) for the vertical, (b) for the anteroposterior, and (c) for the mediolateral directions. Each line is associated with each MWC of the same type.

Overall, no obvious common behaviour was found among all the MWCs. Between one and seven eigenmodes were identified for each MWC. The eigenmodes were identified from 9 to 78 Hz, and the damping ratios were included between 0.8% and 7.5%.

A noticeable result is that, in the vertical direction, except for the first eigenfrequency, the frames of the two lightweight MWCs (MWC01 and MWC02) exhibited similar modal properties. Indeed, the eigenmodes were identified at 35.5 (SD: 0.2) Hz, 44.9 (SD: 1.8), and 63.3 (SD: 3.2) Hz, with damping ratios at 5.0 (SD: 0.5)%, 3.2 (SD: 0.3)%, 2.7 (SD: 0.1)%, and 2.3 (SD: 0.3)%, respectively.

Comparing the MWC types, the sport court MWCs had fewer eigenmodes than the other types along the mediolateral direction (one to three for the sport MWCs, and from two to six for the others). Furthermore, lower damping ratios were found for the racing MWCs (from 0.7% to 4.3%) than for the other MWC types (from 2% and 7.4%), regardless of the direction. The magnitudes of the FRF, however, were higher for the racing MWCs (lower to $0.4 \text{ m}\cdot\text{s}^{-2}\cdot\text{N}^{-1}$) than for the other MWC types (lower to $0.08 \text{ m}\cdot\text{s}^{-2}\cdot\text{N}^{-1}$).

Finally, several MWCs presented a specific structure, conveying a specific modal behaviour. For instance, while the racing MWCs usually presented an empty squared-shape behind the back seat, MWC11 exhibited a full triangle. As a result, MWC11 revealed significantly fewer eigenmodes than the other racing MWCs, especially from 40 to 60 Hz, while the others exhibited between two and four eigenmodes.

3.2. Side Guards

Figure 3 illustrates the co-located FRF and the eigenmodes identified at the side guard of nine MWCs along the mediolateral direction. The daily MWC01 and the sport court MWC07 were not investigated because they have no side guards. For the side guards studied, between one and five eigenmodes were identified per MWC. The eigenmodes were identified from 9 to 77 Hz and the damping ratios were included between 1.4% and 8.8%.

From a structural point of view, most side guards were plate shaped and recessed on at least two sides of the MWC frame. Only for MWC08 and MWC09 were the side guards recessed on one side with two additional recessed points. Regarding the materials, the side guards were made of plastic (MWC03 and MWC04), aluminium (MWC06, MWC07, MWC08, and MWC09), or carbon fibre (MWC02, MWC10, and MWC11). In the next part, for readability purposes, the results are presented as the mean (standard deviation).

Comparing the MWC types, only the racing MWCs presented noticeable modal properties. First, the racing MWCs presented the highest number of eigenmodes in the frequency range studied: five as compared to three for the other MWC types. Two groups were observed inside the racing MWCs: {MWC08; MWC09} and {MWC10; MWC11}. On the one hand, MWC08 and MWC09 presented eigenmodes at about 16.2 (SD: 1.3) Hz, 28.6 (SD: 0.0) Hz, 50.0 (SD: 1.2) Hz, and 59.6 (SD: 1) Hz, with damping ratios at about 5.8 (SD: 0.1)%, 2.0 (SD: 0.2)%, 1.7 (SD: 0.5)%, and 1.9 (SD: 0.0)%. On the other hand, MWC10 and MWC11 showed eigenmodes at about 33.9 (SD: 1.5) Hz, 41.3 (SD: 0.3) Hz, and 53.2 (SD: 1.1) Hz, with damping ratios at about 3.9 (SD: 2.2)%, 2.0 (SD: 0.3)%, and 2.0 (SD: 0.5)%.

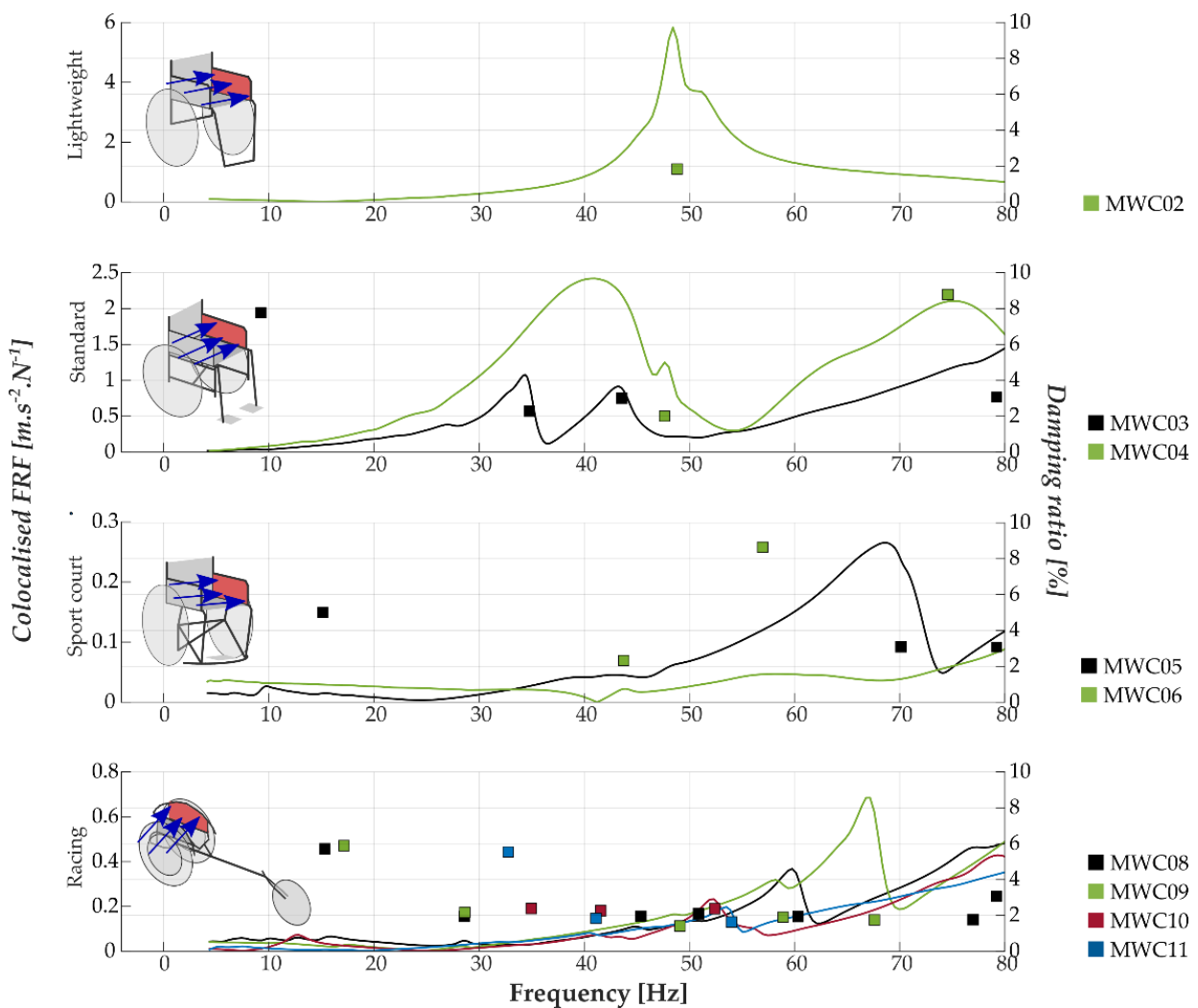


Figure 3. Co-located FRF (lines, associated with the left *y*-axis) and eigenmodes (squared markers, associated with the right *y*-axis) in the mediolateral direction of the side guards for each MWC type studied. Each line is associated with each MWC of the same type.

3.3. Backrest

Figure 4 illustrates the modal properties identified at the backrest of six MWCs along all the directions studied. The sport court MWC07 and all the racing MWCs were not investigated because they have no backrest. For the backrests studied, between one and seven eigenmodes were identified per MWC. The eigenmodes were identified from 8 to 72 Hz, and the damping ratios were included between 1.4% and 11.5%.

Comparing the MWC types, the sport court MWCs showed very few eigenmodes compared to the other MWC types. Specifically, MWC05 reported only two eigenmodes in the mediolateral direction and one eigenmode in the anteroposterior direction. On the other hand, between two and seven eigenmodes were reported for the lightweight and standard MWCs. Interestingly, the eigenmodes were concentrated above 30 Hz for the lightweight MWCs and below 40 Hz for the standard MWCs.

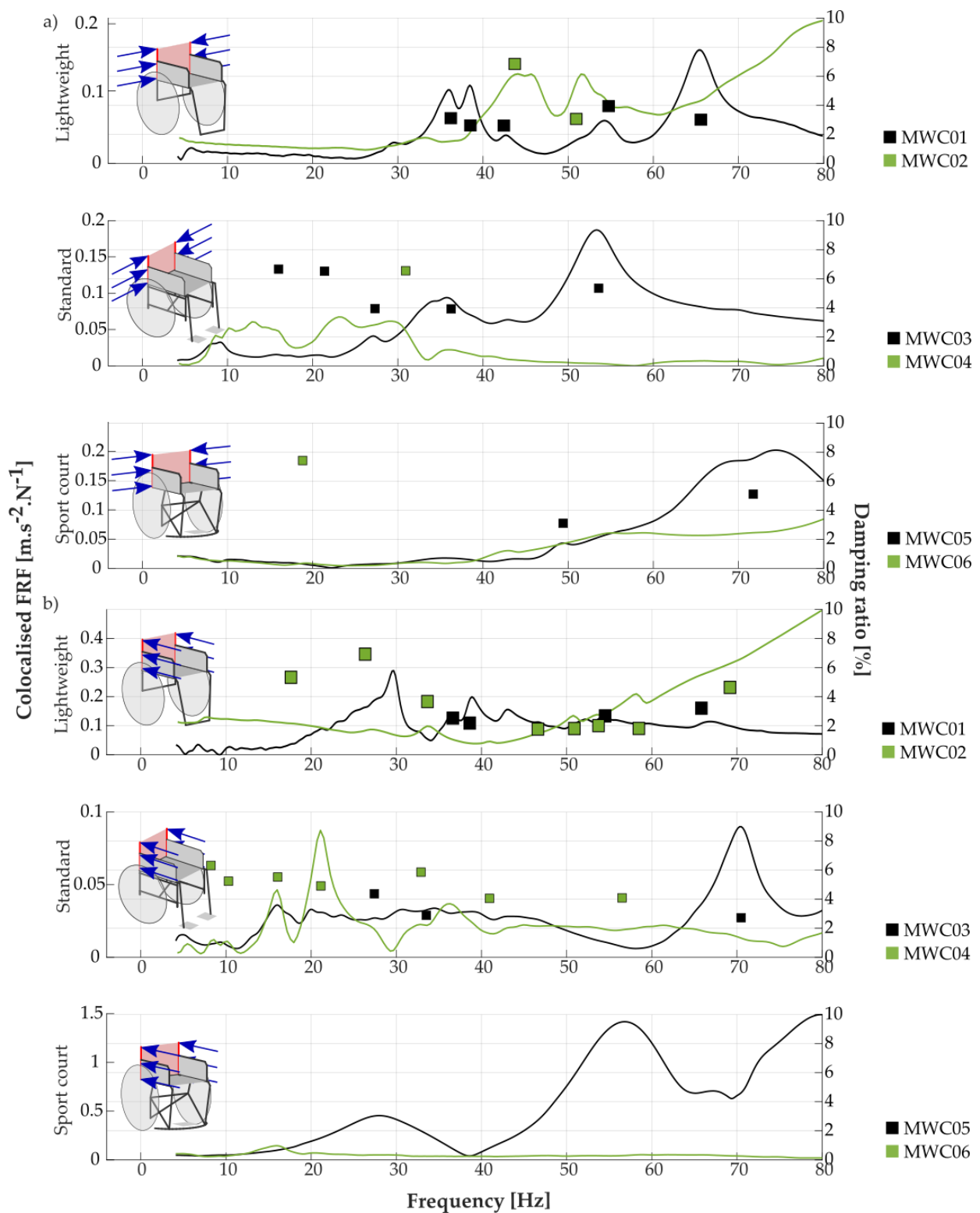


Figure 4. Co-located FRF (lines, associated with the left y -axis) and eigenmodes (squared markers, associated with the right y -axis) of the frame for each MWC type and direction studied (a) for the mediolateral and (b) anteroposterior directions. Each line is associated with each MWC of the same type.

3.4. Seat

Figure 5 illustrates the modal properties identified at the seat of ten MWCs along the vertical direction. The racing MWC08 was not investigated because the two beams on which the tensors were stretched were not accessible in the vertical direction. For the seats studied, between one and five eigenmodes were identified per MWC. The eigenmodes were identified from 6.4 to 74 Hz and the damping ratios were included between 1.4% and 9%

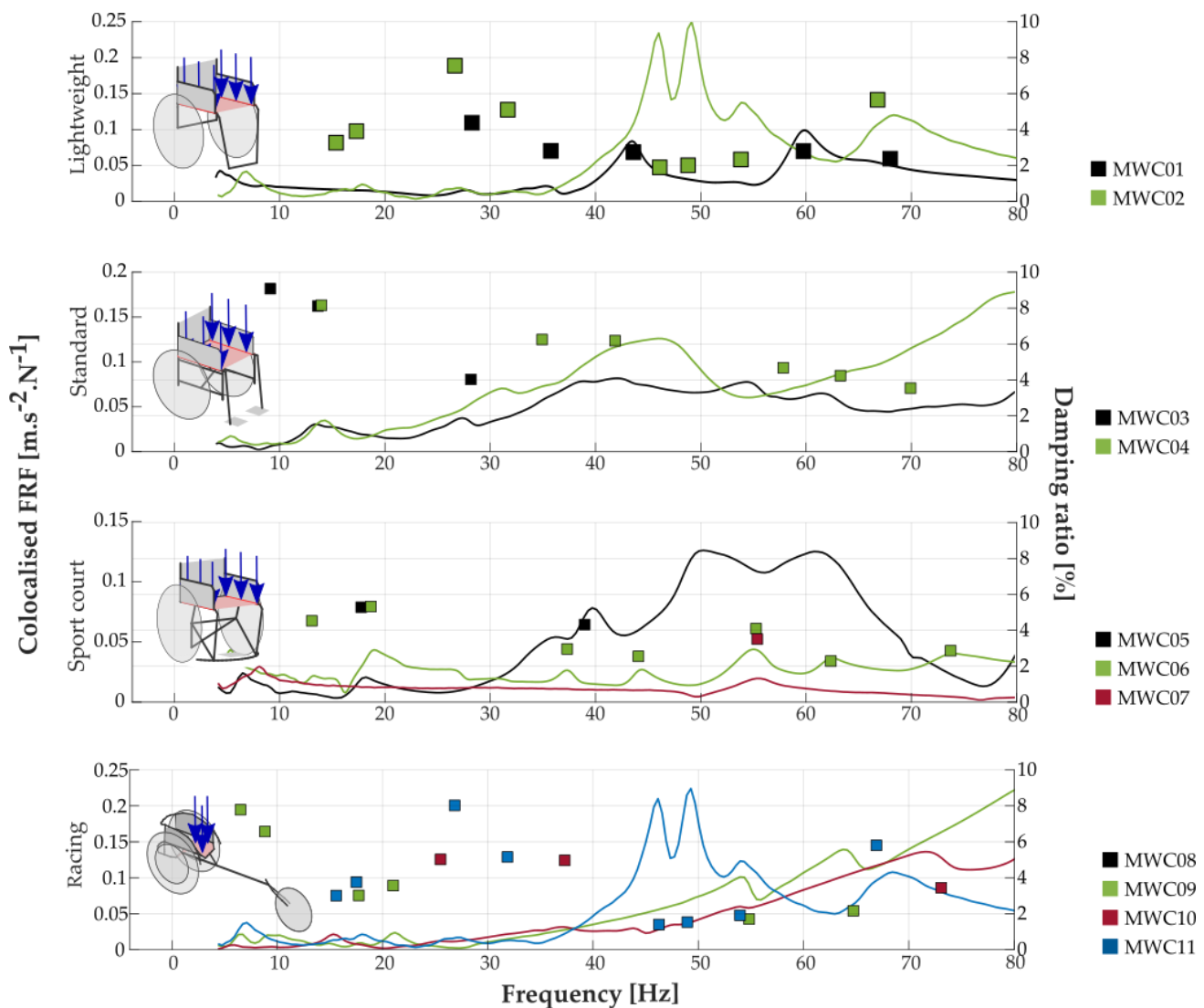


Figure 5. Co-located FRF (lines, associated with the left *y*-axis) and eigenmodes (squared markers, associated with the right *y*-axis) in the vertical direction of the seat for each MWC type studied. Each line is associated with each MWC of the same type.

No straightforward common behaviour was observed among the MWC types. The eigenmodes were identified on the whole frequency range for all the MWC types. In the low frequency (i.e., lower than 40 Hz), all the MWCs reported damping ratios higher than 3%. Interestingly, between 40 and 80 Hz, the standard MWCs reported higher damping ratios (3.4–9%) than the other MWCs (2–5%), especially in the low frequency. Surprisingly, MWC07, for which the seat is a cycle saddle, only showed one eigenmode. For comparison purposes, note that the other MWC seats are made of two beams on which the seat covers are fixed (the lightweight and standard MWCs, the sport court MWC05, and MWC06),

with the rigid plate made of aluminium (the racing MWC08) or carbon fibre (the racing MWC09), or the seat is moulded (the racing MWC10).

3.5. Footrest

Figure 6 illustrates the modal properties identified at the footrest of six MWCs along the vertical direction. The sport court MWC07 and all the racing MWCs were not investigated because they have no footrest. For the footrests studied, between one and six eigenmodes were identified per MWC. The eigenmodes were identified from 11 to 80 Hz, and the damping ratios were included between 2.2% and 7.9%.

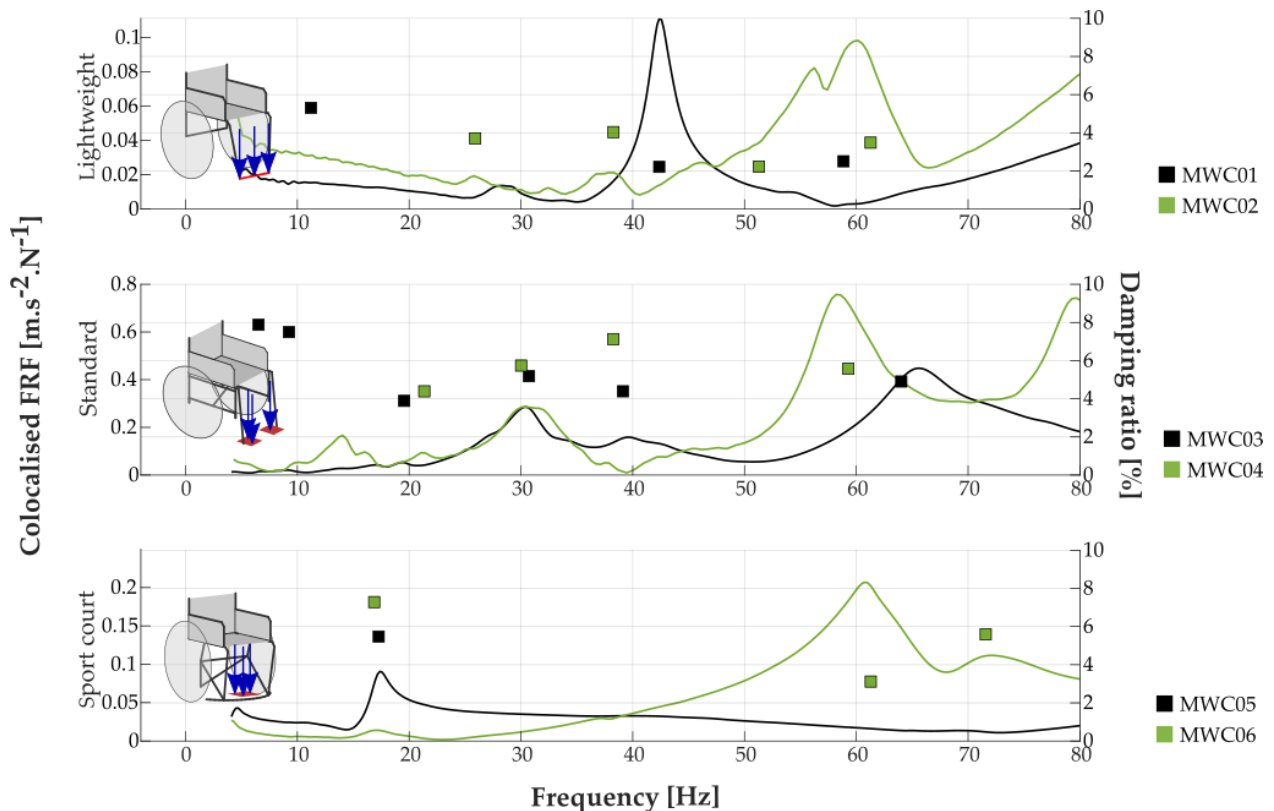


Figure 6. Co-located FRF (lines, associated with the left y -axis) and eigenmodes (squared markers, associated with the right y -axis) in the vertical direction of the footrest for each MWC type studied. Each line is associated with each MWC of the same type.

From a structural point of view, a wide range of footrests was encountered: a metallic plate welded to the frame (the sport MWCs) or integrated into the global MWC frame (the lightweight MWCs), or two plastic plates screwed and clipped to the frame (the standard MWCs). Comparing the MWC types, the only noticeable result was that the sport MWCs presented fewer eigenmodes than the other MWC types (up to three and up to five, respectively).

3.6. Rear Wheel

Figure 7 illustrates the modal properties identified at the rear wheel of ten MWCs along the mediolateral direction. The rear wheel of the standard MWC03 was not studied due to a lack of available time to test all the components of this MWC. For the rear wheel studied, between four and six eigenmodes were identified per MWC. The eigenmodes were identified from 30 to 80 Hz and the damping ratios were included between 1.3% and 4.8%. From a structural point of view, a wide range of rear wheels was encountered: spokes (the lightweight MWC01 and MWC02, the standard MWC03 and MWC04, and the sport court

MWC05 and MWC06), four spokes (the tennis MWC07 and the racing MWC09), or disc (the racing MWC08, MWC10, and MWC11) rear wheels.

Despite the structural differences between the rear wheels studied, a similar FRF amplitude was observed for all the racing rear wheels. Although MWC09 owns four-spokes rear wheels while the others are disc rear wheels, no obvious outcome was pointed out among all the MWCs.

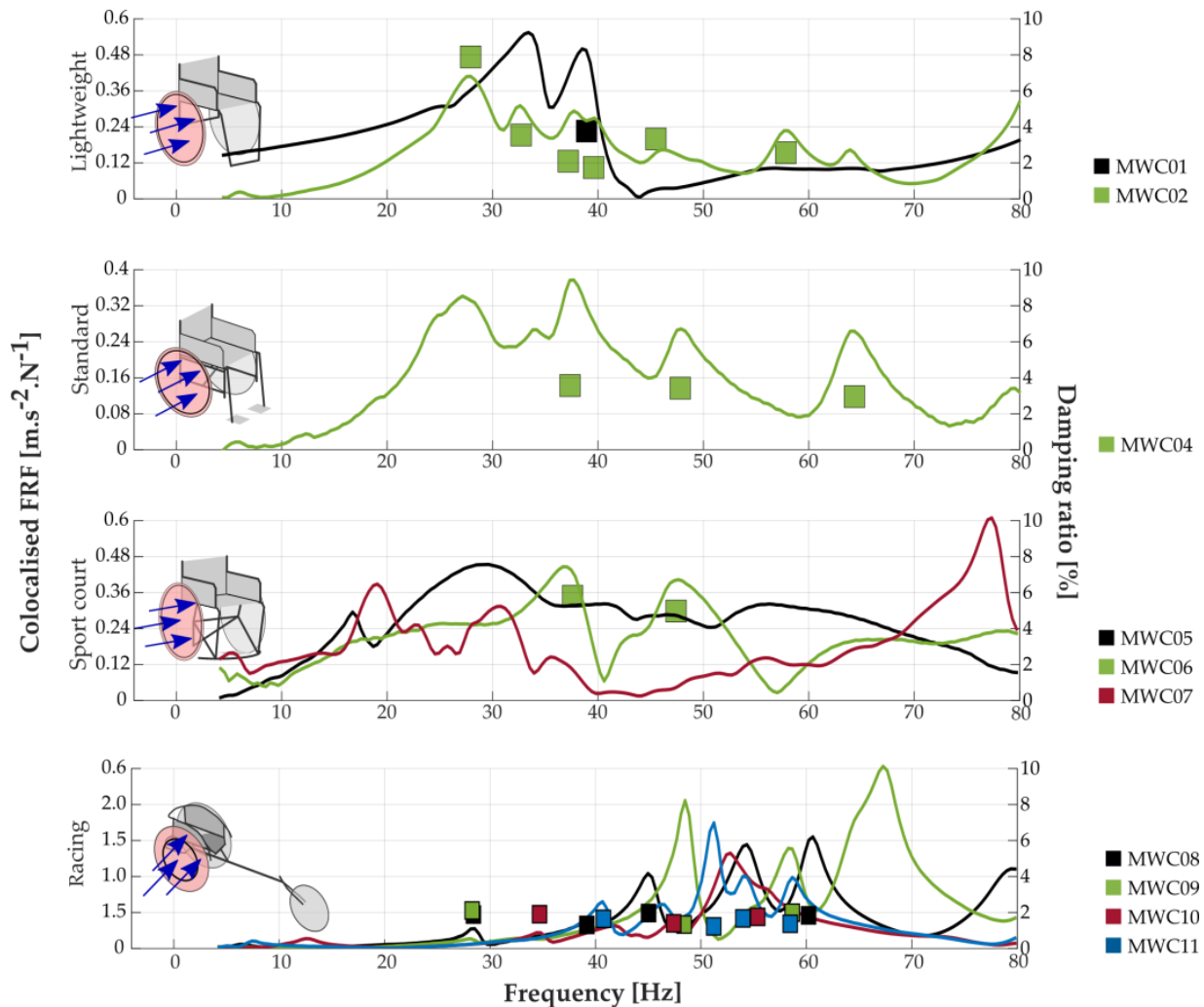


Figure 7. Co-located FRF (lines, associated with the left y -axis) and eigenmodes (squared markers, associated with the right y -axis) in the mediolateral direction of ten MWC wheels. Each line is associated with each MWC of the same type.

3.7. Handrim

Figure 8 illustrates the modal properties identified at the handrims of ten MWCs along the mediolateral direction. The handrims of the sports court MWC07 are not presented because the handrim was included in the rear wheel. For the handrims studied, between four and six eigenmodes were identified per MWC. The eigenmodes were identified from 10 to 80 Hz and the damping ratios were included between 0.2% and 8%.

A higher FRF amplitude was observed for the racing MWCs (i.e., up to $1.6 \text{ m}\cdot\text{s}^{-2}\cdot\text{N}^{-1}$) than the other MWC types (i.e., up to $0.6 \text{ m}\cdot\text{s}^{-2}\cdot\text{N}^{-1}$). Only for the racing MWC09 and MWC11 handrims were the eigenmodes identified between 4 and 80 Hz, and each presented only one eigenmode.

Further, a common behaviour is highlighted throughout the parts and directions of a given MWC. See for instance MWC01, for which an eigenmode was consistently

identified at 42 Hz at the footrest and the seat in the vertical direction; at the backrest in the anterior–posterior direction; and at the frame for both vertical and anteroposterior directions. Additionally, for the racing MWCs, many of the eigenmodes observed on the wheel were also identified at the handrims and the sideguards.

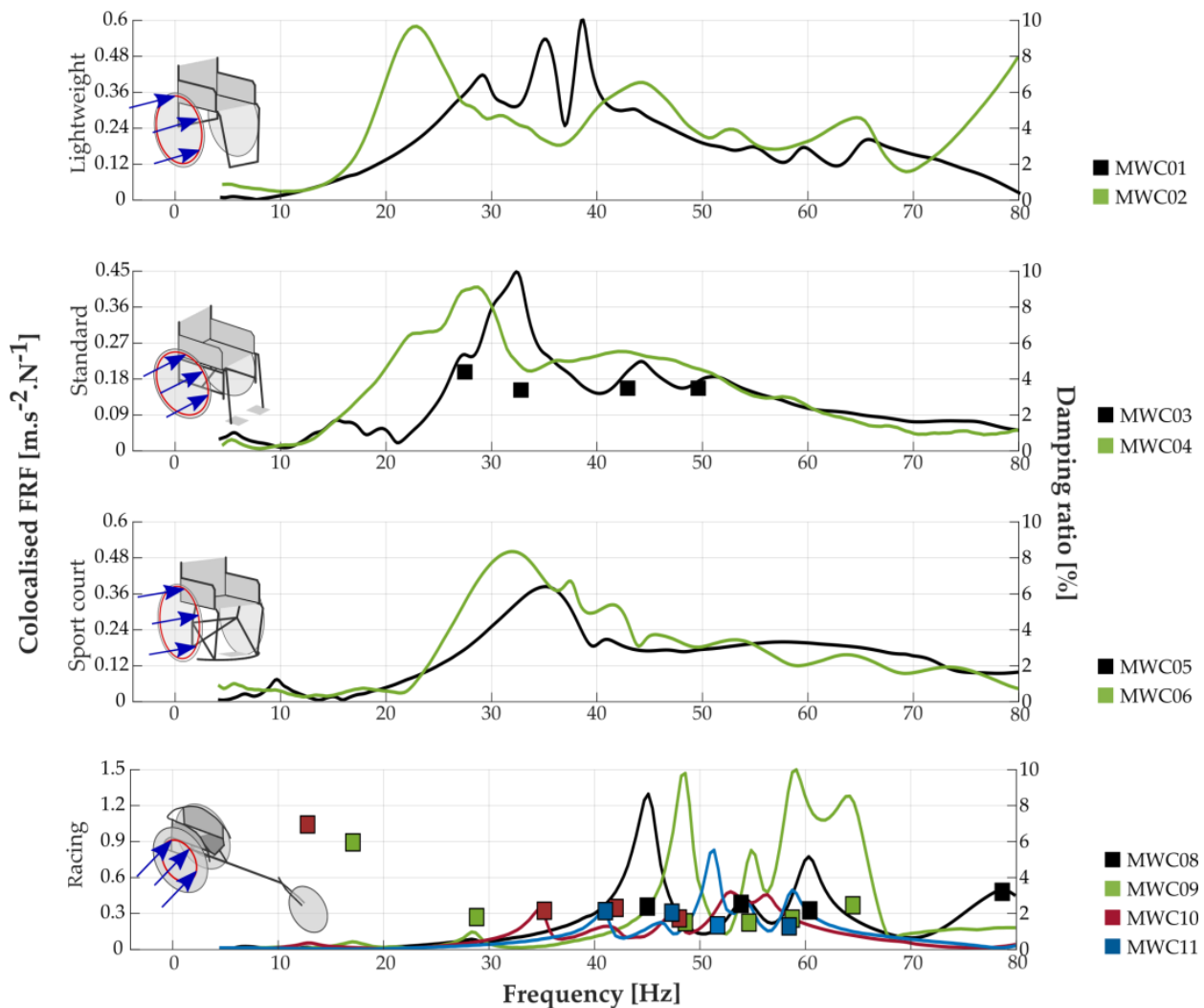


Figure 8. Co-located FRF (lines, associated with the left y -axis) and eigenmodes (squared markers, associated with the right y -axis) in the mediolateral direction of ten MWC handrims. Each line is associated with each MWC of the same type.

4. Discussion

This study aimed at providing an understanding of the dynamical behaviour of eleven MWCs. For this purpose, experimental modal analyses (EMA) in the frequency range known to be deleterious for the human body (i.e., [4–80 Hz] [9]) were performed on lightweight, standard, and sports MWCs. The modal properties of the frame, side guards, backrest, seat, footrest, rear wheel, and handrim were identified and will be discussed below.

Discussing our findings with respect to the literature is difficult since only one publication addressed the dynamical behaviour of standard MWCs [18] and none investigated lightweight or sport MWCs. The approach developed by Skendraoui et al. [18] aimed to develop an MWC numerical model. As a result, Skendraoui et al. [18] chose to report only one or two eigenmodes per MWC part, described solely by eigenfrequencies. Nevertheless, our findings for MWC03 and MWC04, which are standard MWCs, are mostly in agreement

with the data reported by Skendraoui et al. [18]. Indeed, the eigenfrequencies identified for the frame and the footrest matched, while the values reported for the seat differed by about 10 Hz. We hypothesize that the difference is due to the seat design and the use of a cushion in Skendraoui's study. This assumption is supported by the high variability we observed for a given MWC type. Indeed, each MWC owns a unique combination of geometries and materials. Such complex structures preclude a straightforward statement regarding their dynamical behaviour, stressing the need for a dedicated study for each MWC design.

Using the car seat nomenclature [27], the lateral bending mode, fore-aft bending mode, and twisting mode (Figure 9) were identified on the mode shape of the lightweight and standard MWC seat and backrest. These modes occurred at eigenfrequencies comparable to the ones reported by Lo et al. [27]. For the lightweight and standard MWCs, our findings revealed a lateral bending mode, a fore-aft bending mode, and a twisting mode at 34–36 Hz, 39 Hz, and 57–59 Hz, while Lo et al. obtained 24–36 Hz, 33–48 Hz, and 42–62 Hz, respectively [27]. Surprisingly, no lateral mode was identified for the lightweight MWC01. One possible reason is that this mode was omitted or rejected because our mode validation parameters could have been too restrictive. Another possibility is that the mode was outside the frequency range studied for this specific MWC.

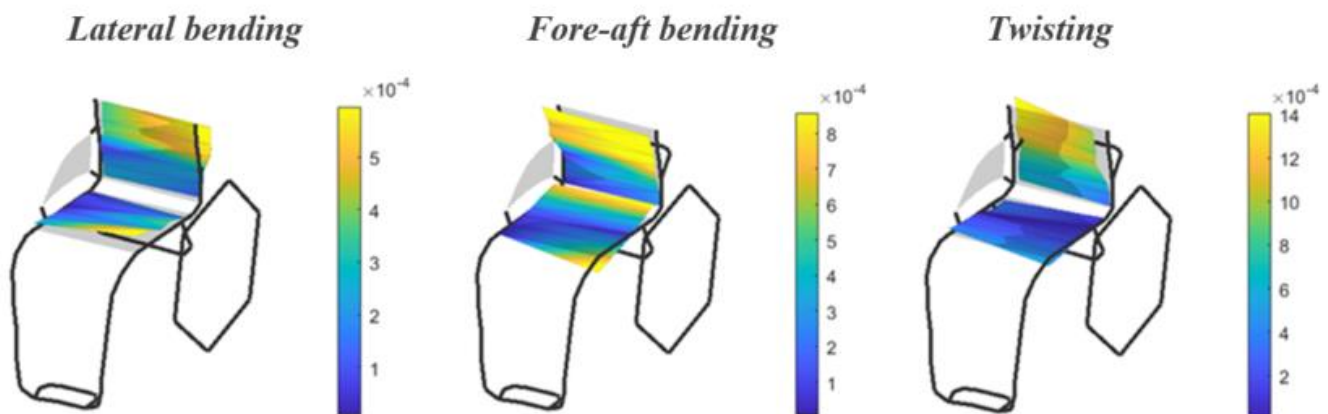


Figure 9. Modal shapes of the seat/backrest system illustrated on the lightweight MWC02. For the visualisation, modes shapes deformation was amplified by a factor of 50.

More generally, the MWC seats presented more than the three cars seat eigenmodes in the [4–80] Hz frequency range. The reason for this difference in the number of identified modes is most likely due to highly different structures. The metallic structure of the car is indeed generally bigger than the MWCs'. Moreover, car seats are closed structures whereas MWC seats are only two parallel metallic beams. The number of MWC eigenmodes is nonetheless comparable to bicycle frames. For bicycles, Champoux et al. [28,29] identified seven eigenmodes for a bicycle with an aluminium frame. Interestingly, our results also suggest that MWC frames dampen vibrations better than bicycle frames (from 0.8% to 7.5% and from 0.2% to 1.8%, respectively). Such differences could be explained by the fact that the MWC is composed of numerous assembled parts, generating a mechanical backlash that reduces the transmission of vibration [30], while a bicycle frame is one welded structure.

Beyond the number of eigenmodes, the eigenfrequency obtained for the MWC07 seat, which is a bicycle saddle (a customized tennis MWC), was consistent with the range of eigenfrequencies reported for bicycles: we identified one eigenmode at 58 Hz. A finite element analysis performed for three saddles with a common design identified first eigenfrequencies from 36 to 140 Hz depending on the saddle design [31]. However, as the MWC07 saddle material (i.e., carbon fibre) and fixation system (i.e., carbon fibre bonding) differed from the bicycle saddle tested (i.e., a common saddle design), a more in-depth comparison would not be relevant.

The results obtained for the spoke wheels were also consistent with the literature. Indeed, for a bicycle spoke wheel, Hou et al. [32] identified the first eigenmode at 90 Hz, which is higher than our range of study.

From the point of view of the user's safety, the experimental modal analyses confirmed the results of Skendraoui et al. [18]: several MWC eigenmodes were identified in the range [4–80] Hz, conveying that an MWC's response to vibration is maximal in the range of frequencies that are deleterious for the human body [9]. As each MWC owns particular dynamical properties, no generic damping system can be developed to reduce the MWC users' exposure to vibrations. This observation underlines the need to accurately assess the modal behaviour of MWCs to preserve users' health. To protect MWC users from the health effects of vibration, the vibration transmission from the MWC to the user should be as low as possible between 4 and 80 Hz, and especially between 4 and 12 Hz, where the risks to the health of the seated human are the greatest [9]. In view of the ground irregularities, it is expected that the excitation generated by MWC propulsion is white noise. All vibration frequencies in the frequency range that is deleterious to the human body must therefore be considered. In addition, although only a few eigenmodes were identified for the wheel and handrim, these MWC parts do not completely dampen vibrations for the frequency range [4–80] Hz. Vibrations at all frequencies could therefore be transmitted to the MWC parts that are in contact to the user. The MWC parts in contact with the user should therefore present as few eigenmodes and/or higher damping ratios as possible in the frequency range that is deleterious for the human body. The results showed that the backrest and footrest of the sports court MWC had the fewest eigenmodes between 4 and 80 Hz. One way to reduce the WBVs transmitted by the MWC to the user would be to take inspiration from existing sports court MWC designs. Further, special attention should be paid to the vibration transmission through the side guards for sport MWCs. Contrary to daily use, athletes are indeed in contact with the side guards during MWC sports practice. According to our results, the side guards of the racing MWCs are those which present the most eigenmodes between 4 and 80 Hz. In order to preserve the health of racing MWC athletes, the side guards of racing MWCs should be improved, reducing this number. MWC seats presented only a few modes lower than 40 Hz or a high damping ratio (higher than 3%). Nonetheless, cushions, which can be understood as a damping element, are usually added to the MWC seat. Articles that investigated vibration transmission through MWC cushions revealed that cushions tend to amplify vibrations at frequencies around 4 Hz for the isolated cushion, and around 8 Hz for cushions loaded by a participant [16]. Therefore, it is all the more important that the MWC seat structure avoid transmitting/amplifying vibrations at frequencies at which cushions amplify the vibration.

One seating system (MWC07, equipped with the bicycle saddle) stands out from the others and has only one eigenmode at 58 Hz. Although such a seat seems to be a good way to prevent MWC users from vibration risks, it cannot be recommended to all MWC users, especially users with weak postural control at the hip and lumbar joints, because of a lack of support (it is currently used by a lower limb amputee).

Obviously, designing an MWC is not only a matter of low frequency vibrations. The conception process needs to account for many constraints: the MWC has to comply with the MWC users' needs, be comfortable, and be safe. For this purpose, the MWC frame's eigenmodes should also be considered. Indeed, such vibrations could generate noise that affects the user's comfort, as well as the MWC structure (e.g., unscrewed elements, micro cracks in the structure). The latter structure concerns are specific to each MWC type. For instance, although only a few elements of racing MWCs are screwed, there is a risk of generating structural micro-cracks, especially considering the high vibration level induced by the high speed of racing MWC practice. Daily MWCs, on the other hand, are mainly constituted of screwed parts and therefore could be affected by the loose screws phenomenon.

The main limitation of the study arises from the complexity and diversity of MWC structures. The modal identification of such 3D systems made of numerous elements

of various materials and mechanical linkages is still a challenge using a roving hammer test [11]. Another limitation is that the study focused on the experimental modal analyses of an empty MWC. Numerous articles have indeed underlined the need to account for the users and an ecological context to assess the equipment's mechanical behaviour [33]. MWC modal properties are thus likely to be affected by the presence of the user and the rolling condition. Articles about bike modal analysis noticed small changes in the eigenfrequencies value, the modes' shapes, and an increase in the damping ratio with the presence of the user on the bike [28]. Future research will gain insights into how the presence of MWC users affects the MWC modal properties under real use conditions through operational modal analysis [34]. Finally, the modal properties obtained in the present study could already be useful to develop a mechanical model or to adjust a finite element model of the MWC.

5. Conclusions

MWC users are, on a daily basis, overexposed to vibrations, implying risks for their health. To reduce the vibration exposures of the MWC users, it is necessary to model MWCs. Such models need dynamical properties of the MWC. In this approach, experimental modal analysis was realized, through hammer roving tests, on eleven MWCs, including daily and sport MWCs. The experimental modal analyses revealed that all MWCs presented eigenmodes at numerous frequencies in the frequency range that is deleterious for the human body (i.e., [4–80 Hz]). However, as each MWC owns particular dynamical properties, it is necessary to characterize them before modelling them. Additionally, no generic damping system can be developed to reduce the MWC user's exposure to vibrations. Nevertheless, this study is the first to compare complete 3D modal analyses of several MWC types and to include sports MWCs. Such results provide the first database that is useful for MWC manufacturers and scientists for MWC model development. Additionally, it provides a valuable source of information for the sizing and design of MWCs with respect to user comfort and health.

Author Contributions: O.L.: conceptualization, methodology, data acquisition, analysis, writing—original draft. D.C.: conceptualization, methodology, data acquisition, analysis, supervision, writing—review and editing. C.S.: conceptualization, methodology, data acquisition, analysis, supervision, writing—review and editing. L.K.: data acquisition. P.T.: supervision, writing—review and editing. All authors have read and agreed to the published version of the manuscript.

Funding: This research was funded by a doctoral allowance from the Université Sorbonne Paris Nord, Paris, France.

Conflicts of Interest: The authors declare no conflict of interest.

Appendix A

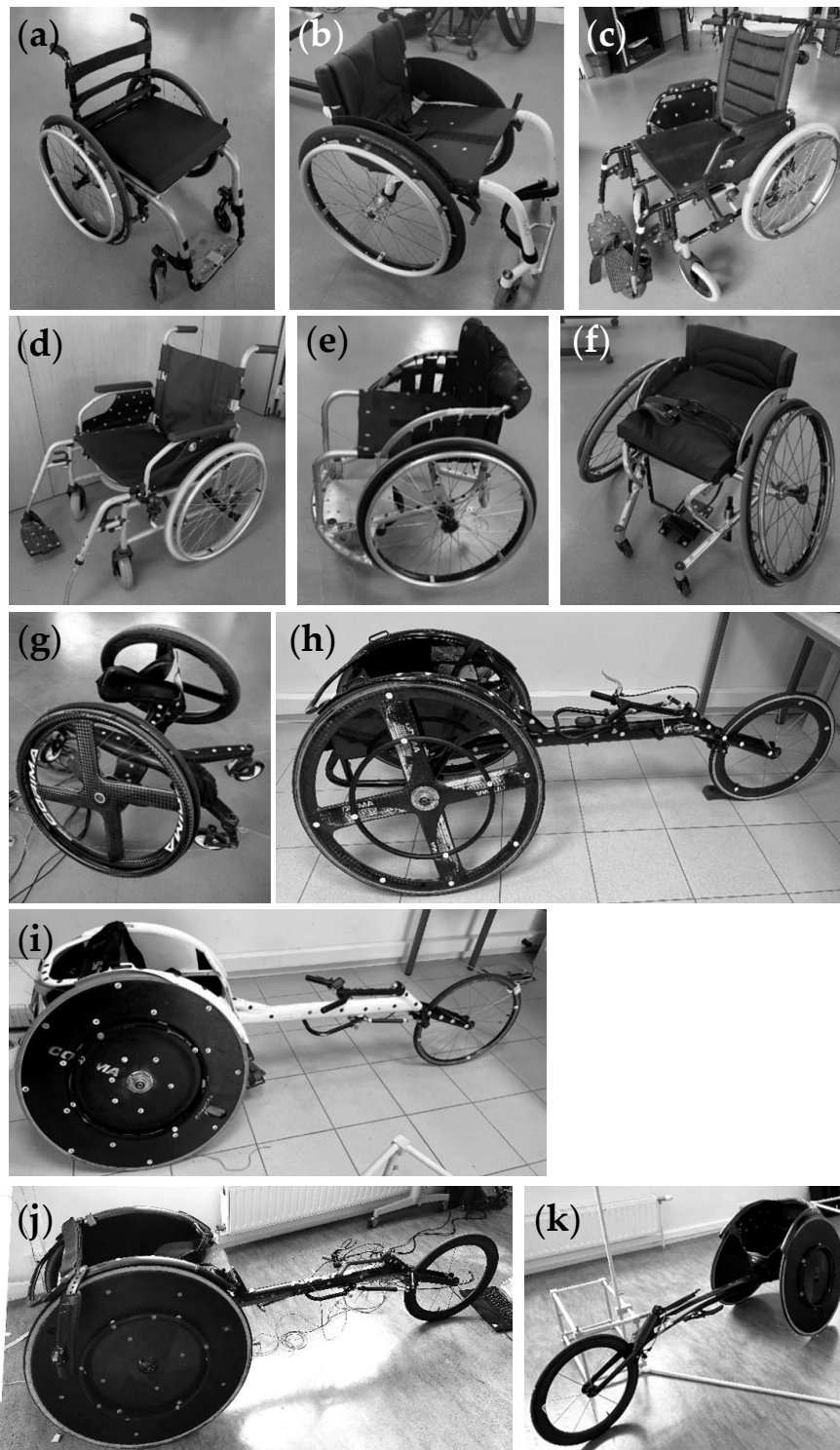


Figure A1. Picture of tested MWCs. (a–k) Lightweight MWC01 and MWC02, standard MWC03 and MWC04, basketball MWC05, tennis MWC06 and MWC07, and racing MWC08, MWC09, MWC10, and MWC11.

References

1. Pope, M.H.; Wilder, D.G.; Magnusson, M.L. A Review of Studies on Seated Whole Body Vibration and Low Back Pain. *Proc. Inst. Mech. Eng. H* **1999**, *213*, 435–446. [CrossRef] [PubMed]
2. Pope, M.H.; Hansson, T.H. Vibration of the Spine and Low Back Pain. *Clin. Orthop. Relat. Res. (1976–2007)* **1992**, *279*, 49–59. [CrossRef]
3. Boninger, M.L.; Cooper, R.A.; Fitzgerald, S.G.; Lin, J.; Cooper, R.; Dicianno, B.; Liu, B. Investigating Neck Pain in Wheelchair Users. *Am. J. Phys. Med. Rehabil.* **2003**, *82*, 197–202. [CrossRef] [PubMed]
4. Dupuis, H.; Zerlett, G. Whole-Body Vibration and Disorders of the Spine. *Int. Arch. Occup. Environ. Health* **1987**, *59*, 323–336. [CrossRef] [PubMed]
5. Newell, G.S.; Mansfield, N.J. Evaluation of Reaction Time Performance and Subjective Workload during Whole-Body Vibration Exposure While Seated in Upright and Twisted Postures with and without Armrests. *Int. J. Ind. Ergon.* **2008**, *38*, 499–508. [CrossRef]
6. Griffin, M.J. *Handbook of Human Vibration*; Griffin, M.J., Ed.; Academic Press: London, UK, 1990; ISBN 978-0-12-303040-5.
7. Nakashima, A. *The Effects of Vibration Frequencies on Physical, Perceptual and Cognitive Performance*; DRDC: Toronto, ON, Canada, 2006; p. 30.
8. European Directive 2002/44/EC—Vibration. 2002. Available online: <https://osha.europa.eu/en/legislation/directives/19> (accessed on 15 July 2022).
9. ISO 2631-1: 2014; Mechanical Vibration and Shock. Part 1: Evaluation of Human Exposure to Whole Body Vibration. International Standards Organization: Geneva, Switzerland, 2014.
10. Garcia-Mendez, Y.; Pearlman, J.L.; Boninger, M.L.; Cooper, R.A. Health Risks of Vibration Exposure to Wheelchair Users in the Community. *J. Spinal. Cord. Med.* **2013**, *36*, 365–375. [CrossRef]
11. Schwarz, B.J.; Richardson, M.H. Experimental modal analysis. *CSI Reliab. Week* **1999**, *35*, 1–12.
12. Piranda, J. Analyse modale expérimentale. *Technique l'ingénieur* **2001**, *32*, 1–29. [CrossRef]
13. Matsuoka, Y.; Kawai, K.; Sato, R. Vibration Simulation Model of Passenger-Wheelchair System in Wheelchair-Accessible Vehicle. *J. Mech. Des.* **2003**, *125*, 779–785. [CrossRef]
14. Lariviere, O.; Chadefaux, D.; Sauret, C.; Thoreux, P. Vibration Transmission during Manual Wheelchair Propulsion: A Systematic Review. *Vibration* **2021**, *4*, 444–481. [CrossRef]
15. Brown, K.; Flashner, H.; McNitt-Gray, J.; Requejo, P. Modeling Wheelchair-Users Undergoing Vibrations. *J. Biomech. Eng.* **2017**, *139*, 094501. [CrossRef] [PubMed]
16. Garcia-Mendez, Y. Dynamic Stiffness and Transmissibility of Commercially Available Wheelchair Cushions Using a Laboratory Test Method. *J. Rehabil. Res. Dev.* **2012**, *49*, 32. [CrossRef] [PubMed]
17. Kawai, K.; Matsuoka, Y. Construction of a Vibration Simulation Model for the Transportation of Wheelchair-Bound Passengers. *SAE Tech. Pap.* **2000**. [CrossRef]
18. Skendraoui, N.; Bogard, F.; Murer, S.; Beaumont, F.; Abbes, B.; Polidori, G.; Nolot, J.-B.; Erre, D.; Odoif, S.; Taiar, R. Experimental Investigations and Finite Element Modelling of the Vibratory Compartment of a Manual Wheelchair. In *Human Systems Engineering and Design*; Ahram, T., Karwowski, W., Taiar, R., Eds.; Advances in Intelligent Systems and Computing; Springer International Publishing: Cham, Switzerland, 2019; Volume 876, pp. 682–688, ISBN 978-3-030-02052-1.
19. Hischke, M.; Reiser, R.F. Effect of Rear Wheel Suspension on Tilt-in-Space Wheelchair Shock and Vibration Attenuation. *PMR* **2018**, *10*, 1040–1050. [CrossRef] [PubMed]
20. Tarabini, M.; Mauri, N.; Gaudio, I.; Cinquemani, S.; Moorhead, A.P.; Bongiovanni, R.; Feletti, F. Hand-Arm Vibration in Motocross: Measurement and Mitigation Actions. *Muscle Ligaments Tendons J.* **2020**, *10*, 280. [CrossRef]
21. DiGiovine, C.P.; Cooper, R.A.; Fitzgerald, S.G.; Boninger, M.L.; Wolf, E.J. Songfeng Guo Whole-Body Vibration during Manual Wheelchair Propulsion with Selected Seat Cushions and Back Supports. *IEEE Trans. Neural. Syst. Rehabil. Eng.* **2003**, *11*, 311–322. [CrossRef]
22. Scislo, L.; Guinchart, M. Non-Invasive Measurements of Ultra-Lightweight Composite Materials Using Laser Doppler Vibrometry System. In Proceedings of the 26th International Congress on Sound and Vibration, ICSV 2019, Montreal, QC, Canada, 7–11 July 2019.
23. Martin, G. *Méthode de Corrélation Calcul/Essai Pour L'analyse du Crissement*; École Nationale Supérieure d'Arts et Métiers: Paris, France, 2017.
24. Loisel, J.; Bascou, J.; Poulet, Y.; Sauret, C. Evaluation of a Simple Characterisation Method of the 3D-Position of a Manual Wheelchair Centre of Mass. *Comput. Methods Biomech. Biomed. Eng.* **2020**, *23*, S172–S174. [CrossRef]
25. Loisel, J.; Poulet, Y.; Bascou, J.; Sauret, C. Evaluation of the Spring-Loaded Turntable Method to Determine the Yaw Mass Moment of Inertia of a Manual Wheelchair. *Comput. Methods Biomech. Biomed. Eng.* **2021**, *24* (Suppl. S1), 288–289.
26. Poulet, Y.; Loisel, J.; Sauret, C. Evaluation of the Direct Linear Transformation Method for the Assessment of Manual Wheelchairs' Configuration. *Comput. Methods Biomech. Biomed. Eng.* **2021**, *24* (Suppl. S1), 286–287.
27. Lo, L.; Fard, M.; Subic, A.; Jazar, R. Structural Dynamic Characterization of a Vehicle Seat Coupled with Human Occupant. *J. Sound Vib.* **2013**, *332*, 1141–1152. [CrossRef]
28. Champoux, Y.; Richard, S.; Drouet, J.-M. Bicycle Structural Dynamics. *Sound Vib.* **2007**, *41*, 16–24.
29. Richard, S. *Etude du Comportement Dynamique d'un vélo de Route en Lien Avec le Confort du Cycliste*; Université de Sherbrooke: Sherbrooke, QC, Canada, 2005.

30. Dalvi, G.; Kumar, P.; Vispute, T.; Jagtap, A.S.R.; Fr, C. Rodrigues Institute of Technology, Navi Mumbai Modal Analysis of Beam Type Structures. *IJERT* **2015**, *V4*, IJERTV4IS040847. [[CrossRef](#)]
31. Cho, J.; Han, M. Study on Structural Durability Analysis at Bicycle Saddle. *Trans. Korean Soc. Automot. Eng.* **2013**, *21*, 104–112. [[CrossRef](#)]
32. Hou, S.S. Design of a Bicycle Wheel with Shock Absorption Ability. *AMM* **2017**, *872*, 235–240. [[CrossRef](#)]
33. Chadeaux, D.; Rao, G.; Le Carrou, J.-L.; Berton, E.; Vigouroux, L. The Effects of Player Grip on the Dynamic Behaviour of a Tennis Racket. *J. Sports Sci.* **2017**, *35*, 1155–1164. [[CrossRef](#)]
34. Au, S.-K. *Operational Modal Analysis*; Springer: Singapore, 2017; ISBN 978-981-10-4117-4.